GaAs Monolithic DC–6.4-GHz Variable-Gain Feedback Amplifier

MASAFUMI SHIGAKI, SHIGERU YOKOGAWA, HIROSHI KURIHARA, AND KATSURA YAMADA

Abstract—**A GaAs dc–6.4-GHz variable-gain two-stage feedback amplifier with 11 dB gain has been developed. The wide bandwidth is achieved by combining a microwave matching circuit with a direct-coupled circuit. This design improves the bandwidth significantly. This circuit also has a reduced chip size. Since no interstage capacitor is necessary, the chip size is only 0.5×1.5 mm^2. Active resistance was used in the second stage feedback circuit for variable gain. Au/WSi self-alignment technology with a 1-μm gate length was used to improve the high-frequency characteristics of the FET.**

I. Introduction

Ultra-wide-band amplifiers are required for gigabit-rate optical systems as well as for microwave communication systems [1]–[3]. We have developed a direct-coupled feedback amplifier without an interstage capacitor for use in these communication systems. This type of circuit is suitable for integration on a small monolithic IC circuit for a frequency range down to dc. To expand the bandwidth, we put a buffer circuit in the feedback loop. This type of two-stage amplifier successfully operated from dc to 1.3 GHz with 18 dB gain [4].

This paper describes the design considerations and performance of a newly developed wide-band GaAs monolithic direct-coupled feedback amplifier combined with a distributed-element network. Wide-band characteristics were achieved by using feedback for the lower frequencies and distributed-element network matching at the high frequencies. Variable gain was achieved by using an active resistance in the second-stage feedback loop. The amplifier has 11 dB gain from dc to 6.4 GHz for a 3-dB bandwidth, and the gain is variable over an 11-dB range. An Au/WSi self-alignment gate process (gate length: 1.1 μm) was used to achieve better performance at microwave frequencies than is possible with a WSi gate (5).

II. FET Model

The Au/WSi self-aligned gate, developed for IC process technology, reduces the gate resistance of the self-aligned gate and provides high performance at microwave frequencies [6]. We made two different FET models. The first was a small-signal equivalent circuit model for RF design, calculated by using S parameters. The second was a SPICE program dynamic equivalent circuit model for dc design, calculated by using dc measurement and S parameters. The I–V characteristics in the SPICE parameter model used the following equation.

$$I_{ds}=\beta W/L\left(V_{gs}-V_{th}\right)^{XR}\left(1+\lambda V_{ds}\right)\tanh\left(\alpha V_{ds}\right) \qquad (1)$$

where V_{th} is the threshold voltage, W is the gate width, L is the gate length, β is 1.125×10^{-4}, λ is 0.889, α is 2.02, XR is 1.406, and L is 1.0 [7].

The main parameters of the small-signal model were $G_m=160$ mS/mm, gate resistance = 0.1 Ω/μm, and gate–source capacitance = 1.2 fF/μm at a gate–source voltage of 0 volt.

Manuscript received January 27, 1987; revised June 1, 1987.

M. Shigaki, H. Kurihara, and K. Yamada are with Fujitsu Laboratories Ltd., Nakahara-Ku, 211 Japan.

S. Yokogawa is with Fujitsu Ltd., Nakahara-Ku, 211 Japan.

IEEE Log Number 8716172.

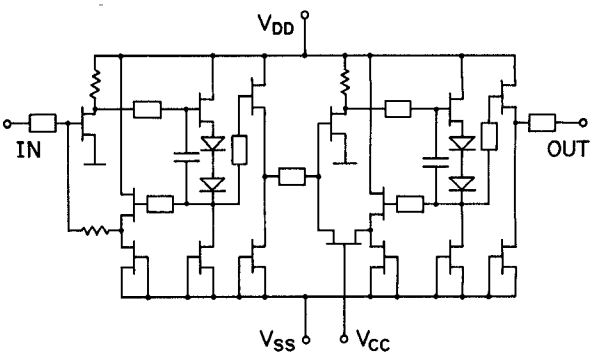

Fig. 1. Two-stage variable-gain wide-band feedback amplifier circuit.

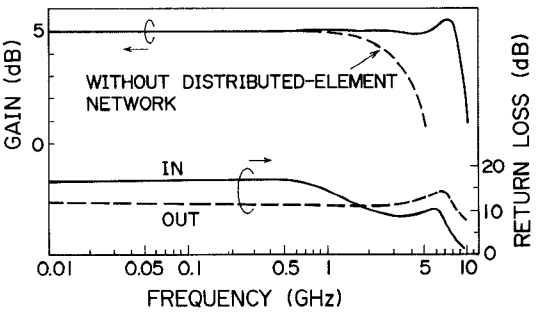

Fig. 2. Simulated characteristics of one-stage wide-band feedback amplifier.

III. Design of the Feedback Amplifier without the Distributed-Element Network

At first we designed a direct-coupled feedback amplifier without the distributed-element network. The object was to adjust the dc level and match the input impedance by a feedback circuit for low frequencies.

Fig. 1 shows the circuit of the two-stage variable-gain feedback amplifier. Since the dc level is adjusted at each stage by a level-shift circuit, this amplifier can operate down to dc. SPICE was used for circuit simulation. A few more circuits and changes of design were added to the previously designed amplifier [4] to obtain wide-band characteristics. First, a buffer circuit was added to the feedback circuit to obtain high impedance at the output of the level-shift circuit. This feedback buffer circuit reduces the load on the level-shift circuit, and achieves better input and output isolation. Second, the gain of the one-stage amplifier was reduced from 10 dB to 5 dB. This gain reduction gave a 500-MHz expansion in the bandwidth. The circuit constants used were as follows. The gate width of the input, output, and level-shift circuits were all 200 μm, and the load resistance of the inverter was 140 Ω. The gate width of the feedback buffer was 40 μm, and the feedback resistance was 80 Ω. The simulated performance of the one-stage amplifier is shown as the dashed line in Fig. 2.

IV. Design of Feedback Amplifier with Distributed-Element Network

A distributed-element network was combined with the direct-coupled feedback amplifier described above to expand the bandwidth at higher frequencies. The S parameter was calculated from the FET equivalent circuits. Suitable circuits were designed for matching each circuit component. Optimization of distrib-

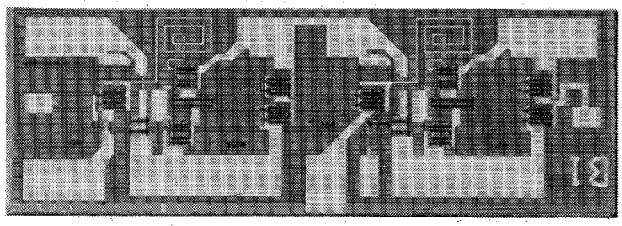

Fig. 3. Photograph of the two-stage wide-band feedback amplifier chip.

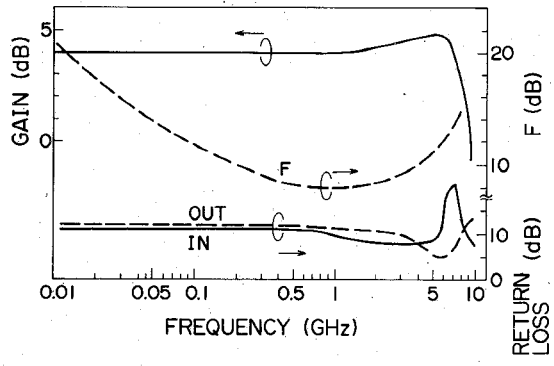

Fig. 4. Characteristics of the one-stage wide-band amplifier.

uted-element parameters was done by the simulation program CAMDI, which was developed in-house.

Short stubs need capacitances for shorting the end of the stub at RF frequencies. Since the capacitance limits the low-frequency characteristics and occupies a large area of the IC chips, this type of stub could not be used in this circuit. Optimization was done to achieve the goal of a 5-dB gain with a 9-GHz bandwidth and 10-dB return loss for the one-stage amplifier. The positions of $S22$ of the input invertor and $S11$ of the level-shift circuit conflicted and were difficult to match. An impedance line of 180 Ω was needed for matching. We put a capacitor of 0.2 pF between input and output of the level-shift circuit to lower the input impedance, allowing us to reduce the matching resistance to 125 Ω. Our first design used some open stubs, but these stubs were eliminated to reduce chip size, with a small sacrifice in gain uniformity. The solid line in Fig. 2 shows the characteristics of the simulated result of the one-stage amplifier with impedance matching using a distributed-element network.

For the two-stage amplifier, we used a FET active feedback resistance in the second stage. Gain is varied by controlling the gate voltage of the FET. Input return loss variations are less than 1 dB when gain is varied, because the input impedance of the circuit is determined mainly by the first stage, which uses fixed feedback resistance.

V. Results for the Fabricated IC

Au/WSi self-aligned gate process was used for fabrication of the newly designed IC. The FET's had 1.1-μm gate length with -1.0 V threshold voltage. Two different amplifiers were fabricated: a one-stage amplifier and a two-stage variable-gain amplifier. The chip size is 0.5 mm×1.0 mm for the one-stage amplifier and 0.5 mm×1.5 mm for the two-stage amplifier, shown as Fig. 3. The supply voltage is ±5.0 V. The IC was mounted on a chip carrier during measurement.

The characteristics of the one-stage amplifier are shown in Fig. 4. Gain was 4 dB from dc to 8.4 GHz at 3 dB down referred to the dc gain. Input return loss is over 8 dB within the bandwidth, but the output return loss is 5 dB. The best noise figure is 8 dB,

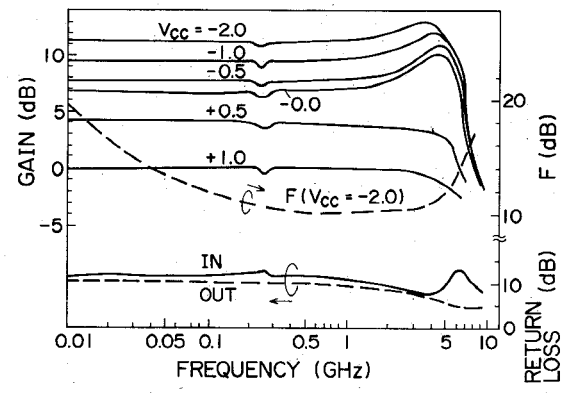

Fig. 5. Frequency characteristics of the two-stage variable-gain wide-band feedback amplifier.

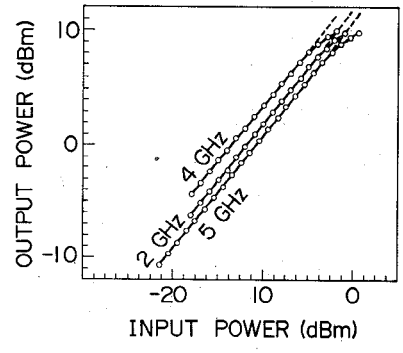

Fig. 6. Input and output characteristics of the two-stage variable-gain wide-band feedback amplifier.

and the noise increases at low frequencies as a result of the $1/f$ noise influence. Power consumption is 700 mW.

The characteristics of the two-stage variable-gain amplifier are shown in Figs. 5 and 6. This amplifier has 11.2 dB gain from dc to 6.4 GHz. The variable-gain limit is 11 dB for a control voltage from -2.0 V to 1.0 V. Input return loss is over 8 dB within the bandwidth, and output return loss is 5 dB. Input and output return loss vary less than 1 dB when gain is changed. The best noise figure is 10 dB. Output power is 9 dBm at 1 dB gain compression. Power consumption is 1.6 W. The gain dip at 250 MHz was caused by the V_{DD} bias circuit. This can be eliminated by using a 50-Ω absorbing resistance outside the IC chip. Over the ±4.5 V bias condition, this characteristic could be obtained with less than 0.8 dB fluctuation. The gain drift with temperature was -0.033 dB/°C.

The characteristics are close to the design. However, output return loss is less above 4 GHz than was simulated. This is due to incorrect estimates for the spiral transmission line value and drain conductance of the FET. Better characteristics will be obtained by improvements in design and process.

VI. Summary

A GaAs monolithic ultra-wide-band variable-gain amplifier was designed and fabricated by combining a distributed-element network with a direct-coupled feedback amplifier. This amplifier has a 4-dB gain over a dc-to-8.4-GHz bandwidth for the one-stage amplifier, and an 11.2-dB gain over a dc-to-6.4-GHz bandwidth for the two-stage amplifier. The 11-dB variable gain was achieved by using active feedback resistance. This proves that the circuit technology for combining a direct-coupled amplifier and a distributed-element network is effective for expanding the bandwidth.

ACKNOWLEDGMENT

The authors are grateful to Messrs. Fukuta, Nishi, Izumi, and Ashida, who encouraged them in this study.

REFERENCES

[1] W. C. Petersen, D. R. Decker, A. K. Gupta, J. Dully, and D. R. Chen, "A monolithic GaAs 0 1 to 10 GHz amplifier," in *IEEE MTT-S Int Microwave Symp. Dig.*, 1981, pp. 354–355.
[2] K. Honjo and T. Sugiura, "Microwave broadband GaAs monolithic amplifier," Tech. Rep. IECEJ Japan, MM82-31, pp. 27–33, 1983
[3] I. Bahly, E. Griffin, W. Powell, and C. Ring, "A high speed GaAs monolithic transimpedance amplifier," in *IEEE MTT-S Monolithic Circuits Symp. Dig*, 1986, pp. 35–38.
[4] M. Shigaki, T. Nakamura, and S Yokogawa, "GaAs monolithic buffered feedback amplifier using Au/WSi gate," *Nat. Conf. Record, Semiconductor Devices and Materials*, IECE Japan, 1985, pp. 1–78.
[5] T. Ohnishi, N. Yokoyama, H. Onodera, S. Suzuki, and A. Shibatomi, "Characterization of WSi/GaAs Schottky contacts," *Appl. Phys. Lett.*, vol. 43, p. 588, 1983.
[6] K. Imamura, T. Ohnishi, M. Shigaki, and N. Yokoyama, "Au/TiN/WSi gate self-aligned GaAs MESFETs using rapid thermal annealing method," *Electron. Lett.*, vol. 21, no. 18, 1985.
[7] M. Shigaki, Y. Daido, Y. Takeda, K. Imamura, and H. Suzuki, "5 GHz monolithic astable multivibrator type voltage controlled oscillator," *Trans Inst. Electron. Commun. Eng. Japan*, vol E67, no. 3, pp 161–165, 1984.

A Quasi-Static Analysis of Open-Ended Coaxial Lines

DEVENDRA K. MISRA, MEMBER, IEEE

***Abstract*—A quasi-static analysis of an open-ended coaxial line terminated by a semi-infinite medium on ground plane is presented in this paper. The analysis is based on a variation formulation of the problem. A comparison of results obtained by this method with the experimental and the other theoretical approaches shows an excellent agreement. This analysis is expected to be helpful in the inverse problem of calculating the permittivity of materials *in vivo* for a given input impedance of the coaxial line.**

I. INTRODUCTION

Open-ended coaxial lines have attracted many researchers recently for their application in nondestructive measurements of the complex permittivity of materials. These techniques are very attractive, particularly for *in vivo* measurements of biological materials [1]. Open-circuited air-filled coaxial lines are also used as calibration standards for microwave measurements [2], [3]. For nondestructive measurement of permittivity, the open end of coaxial line is terminated by the sample material, and the input reflection coefficient of the system is measured at a desired frequency and temperature. These data can be related to the complex permittivity of the material. However, this latter part of the problem is not simple and attempts have been made to devise a scheme to do this job.

In one of the approaches for relating the reflection coefficient to the permittivity of the material terminating the coaxial line, nomograms are generated for SR7 coaxial cable at 1 GHz, 3 GHz, and 10 GHz [4]. The complex permittivity of the material is determined from these nomograms for a given reflection coefficient. Obviously, many more nomograms are necessary to cover different frequencies and the coaxial cables, which is not possible in practice. Another approach, in which a lumped equivalent circuit is used for relating the admittance of the sensor to the permittivity, requires the equivalent circuit parameters of the sensor [5]. Initially, these parameters were either measured directly or inferred from measurements on known dielectrics. Static fringing capacitances were calculated later by Gajda and Stuchly using two different computation techniques, viz. The finite-element method (FEM) and the method of moments (MoM) [6].

This paper is based on a stationary formulation of the input admittance of coaxial line terminated by a semi-infinite medium on ground plane. These results are first compared with the data calculated by considering the presence of higher order modes [4]. This formulation is then simplified for a quasi-static case. Static as well as frequency-dependent capacitances are calculated and compared with the available theoretical and experimental data.

II. FORMULATION OF THE PROBLEM

A coaxial line of inner radius a and outer radius b has a flat conducting flange extending to infinity as shown in Fig. 1. The insulation of the line is lossless and homogeneous with relative permittivity ϵ_c. The medium over the ground plane is a linear, isotropic, homogeneous, nonmagnetic material with complex permittivity ϵ^*.

A TEM wave incident on the annular opening through the coaxial line is partially reflected back, with a part of it transmitted into the terminating material. Also, it generates a number of higher order modes over the aperture. The incident TEM mode has no angular variations and has only a magnetic field component H_ϕ along the azimuthal direction ϕ, and an electric field component E_ρ along the radial direction ρ. The fields generated by the incident TEM wave exhibit no variations in angular direction. An expression for the magnetic field intensity $H_\phi(\rho, z)$ in the medium over the ground plane can be obtained by a combination of the equivalence principle and the image theory as follows [7]:

$$H_\phi(\rho, z) = \frac{j\omega\epsilon^*}{\pi} \int_a^b \int_0^\pi E_\rho(\rho', 0)\, \rho' \cos\phi' \frac{\exp(-jkR)}{R}\, d\rho'\, d\phi' \tag{1}$$

where

$$\epsilon^* = \epsilon - j\frac{\sigma}{\omega} \tag{2}$$

$$R^2 = \left[\rho^2 + \rho'^2 + (z - z')^2 - 2\rho\rho' \cos\phi'\right]^2 \tag{3}$$

$$k^2 = \omega^2 \mu_0 \epsilon^*. \tag{4}$$

$E_\rho(\rho', 0)$ is the radial electric field intensity over the aperture, and ϵ and σ represent the permittivity and conductivity of the medium, respectively. As usual, the primed coordinates are used for the source point, and the unprimed coordinates are for the field point. Also, the time harmonic variation $\exp(j\omega t)$ is used for the fields.

The ϕ symmetrical magnetic fields in the coaxial line can be expressed as [7]

$$H\phi(\rho, z) = \frac{A_0}{\rho}\left[\exp(-jk_c z) - \Gamma \exp(jk_c z)\right] + \sum_{\eta=1}^{\infty} A_\eta R_\eta(\rho) \exp(\gamma_\eta z) \tag{5}$$

Manuscript received March 20, 1987; revised May 22, 1987. This work was supported by a grant from the Graduate School, University of Wisconsin at Milwaukee.

The author is with the Department of Electrical Engineering and Computer Science, College of Engineering and Applied Science, University of Wisconsin at Milwaukee, P O. Box 784, Milwaukee, WI 53201.

IEEE Log Number 8716176.